# Roberge-Weiss endpoint in $N_f = 2$ QCD

Claudio Bonati,[1] Guido Cossu,[2] Massimo D'Elia,[3] and Francesco Sanfilippo[4]

[1]*Dipartimento di Fisica, Università di Pisa and INFN, Sezione di Pisa, Largo Pontecorvo 3, 56127 Pisa, Italy*
[2]*Theory Center, IPNS, High Energy Accelerator Research Organization (KEK), Tsukuba 305-0801, Japan*
[3]*Dipartimento di Fisica, Università di Genova and INFN, Sezione di Genova, Via Dodecaneso 33, 16146 Genova, Italy*
[4]*Dipartimento di Fisica, Università di Roma "La Sapienza" and INFN, Sezione di Roma, Piazzale A. Moro 5, 00185 Roma, Italy*

We present the results of extensive simulations regarding the critical behavior at the endpoint of the Roberge-Weiss transition for $N_f = 2$ QCD. We confirm early evidence, presented in Ref. [M. D'Elia and F. Sanfilippo, Phys. Rev. D **80**, 111501(R) (2009).], according to which the Roberge-Weiss endpoint is first order in the limit of large or small quark masses, and second order for intermediate masses. A systematic study of the transition strength as a function of the quark mass in the first order regions, permits us to estimate the tricritical values of the quark mass separating the second order region from the first order ones.

## I. INTRODUCTION

A full understanding of the QCD phase diagram at finite temperature $T$ and baryon chemical potential $\mu_B$ is one of the main unreached goals within the standard model of particle physics. Various questions remain open, which are of fundamental importance both theoretically and phenomenologically, for astrophysics and heavy ion collisions, like the existence and location of a possible critical endpoint in the $T - \mu_B$ plane, accessible to experiments.

Lattice QCD simulations, which are in principle the ideal tool for a full nonperturbative investigation of the phase diagram, are unfortunately hindered at $\mu_B \neq 0$ by the complex nature of the path integral measure (sign problem). Among other approximate methods, a way to partially overcome the sign problem is to consider a purely imaginary quark chemical potential, $\mu_q \equiv \mu_B/3 = i\mu_I$: numerical simulations are feasible and information about real $\mu_B$ can be recovered by analytic continuation techniques [1–15].

Recent literature has pointed out that the phase structure at finite $T$ and imaginary chemical potential may be important by its own, and teach us something about the nonperturbative properties of QCD also at zero or small real $\mu_B$ [10,16–20]. Such phase structure is characterized by a periodicity of the partition function

$$Z(T, \mu_I) = \mathrm{Tr}(e^{-(1/T)(\hat{\mathcal{H}}_{\mathrm{QCD}} - i\mu_I \hat{N}_q)}) \qquad (1)$$

in the angular variable $\theta = \mu_I/T$, which can be viewed, in the path integral representation of the partition function, as a phase rotation of fermion boundary conditions in the Euclidean temporal direction. It can be shown [21] that the period in $\theta$ is $2\pi/N_c$, where $N_c$ is the number of colors. Such periodicity is smoothly realized in the low temperature, confined phase, as expected from the fact that only uncolored states, with $N_q$ multiple of $N_c$, contribute to the system dynamics.

The situation is different in the high temperature phase, as expected from the fact that also colored states appear. Indeed, as can be explicitly verified by perturbative computations [21], the periodicity is realized in a nonanalytic way: the system goes through first order lines, known as Roberge-Weiss (RW) transitions, when $\theta$ crosses some fixed values, $\theta_k = (2k + 1)\pi/N_c$, where $k$ is an integer. For such values of $\theta$ the system possesses an exact $Z_2$ symmetry, which is spontaneously broken for $T > T_{\mathrm{RW}}$ and unbroken for $T < T_{\mathrm{RW}}$: therefore at $T = T_{\mathrm{RW}}$, which is in fact the endpoint of the RW lines, a genuine finite $T$ phase transition takes place for all values of the quark masses. Such transition coincides with the phase transition at which charge symmetry is spontaneously broken when a spatial dimension is compactified below a given critical size (see e.g. Refs. [22–26] for early lattice studies of such transition, which has been investigated in the context of orientifold planar equivalence [27,28]).

The endpoint of the RW lines has been considered by recent literature [10,16,17,19,20,29], for its possible influence on the critical properties and on the phase diagram of QCD. The endpoint can be second order in the 3D Ising universality class, or first order; in the latter case it is actually a triple point, from which two further first order lines depart.

In Ref. [16] first evidence has been presented showing that, for QCD with two degenerate flavors ($N_f = 2$), the endpoint is first order in the limit of small quark masses and second order for intermediate masses; first order comes back in the high quark mass regime, where the system reaches its quenched limit. In the same paper it has been pointed out that, when the endpoint is first order (triple point), one of the further first order lines departing from it can be identified with (part of) the continuation of the critical line to imaginary chemical potential, thus explaining early evidence [3,4] that the latter meets the RW line right on its endpoint. A further conjecture, put forward in

Ref. [16], has been that the nature of the transition at $\mu = 0$ as a function of the quark mass spectrum (which is summarized in the so-called Columbia plot) is regulated by the physics of the RW endpoint itself, i.e. that the $\mu = 0$ transition is first order only when the first order line departing from the RW triple point reaches the $\mu = 0$ axis.

Recently the numerical study of the RW endpoint has been extended to $N_f = 3$ QCD [19], confirming also for this case the presence of a first order transition for small and high quark masses, with a second order region for intermediate masses. Moreover, the authors of Ref. [19] have suggested that the tricritical behavior which is present at the two tricritical masses, separating the second order from the first order regions, may shape the critical line also for real values of the chemical potential, implying a weakening of the transition with real chemical potentials which was suggested also by earlier works [30].

All the results and conjectures above call for a more systematic study of the phase diagram in the $T - \mu_I$ plane, which is perfectly feasible with present simulation algorithms. The aim of the present work is to move a step in this direction, by extending in a substantial way the original results presented in Ref. [16] for $N_f = 2$ QCD. In particular we will present results about the critical behavior at the RW endpoint for a large set of quark masses, confirming the results of Ref. [16] and giving an estimate for the two tricritical masses, $m_{t1}$ and $m_{t2} > m_{t1}$, separating the first order regions from the second order one.

Our first instrument to discern the critical behavior around the RW endpoint is the finite size scaling of various susceptibilities. However, an accurate determination of the critical properties around the tricritical point may be a nontrivial task. Much can be learned in this direction by the study of simpler statistical systems, like the 3D 3-state Potts model in presence of a negative magnetic field $h$ [31,32], which shares some of the properties of QCD along the RW lines, i.e. the presence of a residual $Z_2$ symmetry which gets spontaneously broken at a critical temperature. In that model the transition is first order for small values of $|h|$ and second order for large values of $|h|$, with a tricritical value of the field, $h_{tric}$, separating the two regimes.[1] As shown in Ref. [31], discerning the correct universality class close to $h_{tric}$ is difficult since, at a given distance from $h_{tric}$, tricritical scaling will mask the correct critical indexes up to a given lattice size $L_{max}$, which is regulated by tricritical crossover exponents. A similar phenomenon is expected around $m_{t1}$ and $m_{t2}$. Following Ref. [31], an alternative strategy will be to determine parameters which fix the strength of the first order transition for $m < m_{t1}$ or $m > m_{t2}$, like the latent heat or the gap of the order

parameter, and extrapolate the values of $m$ at which such parameters vanish, i.e. the first order transition disappears.

Our results have been obtained using standard rooted staggered fermions on lattices with $N_t = 4$. The paper is organized as follows: in Sec. II we give more details about the discretized version of QCD under investigation and about the observables and the strategy used for the study of the critical behavior; in Sec. III we present our numerical results and finally, in Sec. IV, we discuss our conclusions and perspectives.

## II. NUMERICAL SETUP

We shall consider the partition function of $N_f = 2$ QCD in presence of an imaginary chemical potential and in the standard staggered discretization of dynamical fermions,

$$Z(T, \theta) \equiv \int \mathcal{D}U e^{-S_G[U]} (\det M[U, \theta])^{1/2}, \qquad (2)$$

where $\theta = \mu_I/T$, $S_G$ is the pure gauge plaquette action and $M$ is the fermion matrix

$$M_{i,j} = am\delta_{i,j} + \frac{1}{2} \sum_{\nu=1}^{3} \eta_{i,\nu}(U_{i,\nu}\delta_{i,j-\hat{\nu}} - U_{i-\hat{\nu},\nu}^{\dagger}\delta_{i,j+\hat{\nu}})$$
$$+ \eta_{i,4}(e^{ia\mu_I}U_{i,4}\delta_{i,j-\hat{4}} - e^{-ia\mu_I}U_{i-\hat{4},4}^{\dagger}\delta_{i,j+\hat{4}}). \qquad (3)$$

Here $i$ and $j$ refer to lattice sites, $\hat{\nu}$ is a unit vector on the lattice, $\eta_{i,\nu}$ are the staggered phases, $a$ is the lattice spacing and $m$ is the bare quark mass.

RW transitions take place for $\theta = (2k + 1)\pi/3$. We shall consider, in particular, the case $\theta = \pi$: for this value the residual $Z_2$ symmetry, which is spontaneously broken at $T_{RW}$, corresponds to charge conjugation, hence the imaginary part of the Polyakov loop or, alternatively, the imaginary part of the baryon number can be taken as possible order parameters; as in Ref. [16], we shall consider the former. In the following $L$ will stand for the spatially averaged Polyakov loop trace (normalized by $N_c$), hence $\mathrm{Im}(L)$ is the order parameter.

The order parameter susceptibility is defined by

$$\chi \equiv L_s^3(\langle \mathrm{Im}(L)^2 \rangle - \langle |\mathrm{Im}(L)| \rangle^2), \qquad (4)$$

where $L_s$ is the spatial size in lattice units, and is expected to scale, around the transition, as follows:

$$\chi = L_s^{\gamma/\nu} \phi(tL_s^{1/\nu}), \qquad (5)$$

where $t = (T - T_{RW})/T_{RW}$ is the reduced temperature. That means that the quantities $\chi/L_s^{\gamma/\nu}$, measured on different lattice sizes, should fall on the same curve when plotted against $\tau L_s^{1/\nu}$.

Another relevant quantity is the specific heat $C$ of the system, which is instead expected to scale as

$$C = C_0 + L_s^{\alpha/\nu} \phi_2(tL_s^{1/\nu}), \qquad (6)$$

where $C_0$ is a regular contribution. The values of the critical indexes $\alpha$, $\gamma$ and $\nu$ which are relevant to our

---

[1] In the Potts model, of course, one does not observe the restrengthening of the transition (hence a second tricritical point), which is present for QCD at low masses and which is likely caused by the interplay with chiral degrees of freedom.

analysis are listed in Table I (see e.g. Refs. [33,34]), together with the values they take for the different critical behaviors which may take place in our system, i.e. first order, second order in the universality class of the 3D Ising model, and tricritical mean field.

A careful verification of Eqs. (5) and (6), as well as of similar relations giving the finite size scaling behavior of other relevant quantities, gives information about critical indexes, hence about the universality class of the transition. A more direct way, in the case of a first order transition, is to verify the existence, in the thermodynamical limit, of finite gaps in the order parameter or in the internal energy (latent heat), which may be visible by looking at double peak distributions of physical observables around the transition, or by studying the large volume limit of some cumulants.

An example is the Binder-Challa-Landau cumulant [35] of the energy, which is defined as $B_4 = 1 - \langle E^4 \rangle / (3 \langle E^2 \rangle^2)$. It can be shown (see e.g. [36]) that near a transition $B_4$ develops minima whose depth scales as

$$B_4|_{\min} = \frac{2}{3} - \frac{1}{12}\left(\frac{E_+}{E_-} - \frac{E_-}{E_+}\right)^2 + O(L_s^{-3})$$

$$= \frac{2}{3} - \frac{1}{3}\left(\frac{\Delta_E}{\epsilon}\right)^2 + O(\Delta_E^3) + O(L_s^{-3}) \qquad (7)$$

where $E_\pm = \lim_{\beta \to \beta_c^\pm} \langle E \rangle$, $\Delta_E = E_+ - E_-$ and $\epsilon = \frac{1}{2}(E_+ + E_-)$. In particular, the thermodynamical limit of $B|_{\min}$ is less than $2/3$ if and only if a latent heat is present. To simplify our analysis we have considered the average plaquette (sum of the spatial and temporal plaquettes) in place of the internal energy, since it is a quantity which can be measured much more easily and, like the internal energy, is even under the $Z_2$ symmetry which gets broken at the RW endpoint. To simplify the notation, in the following we will use the shorthand

$$B = \frac{2}{3} - B_4|_{\min} \qquad (8)$$

and from Eq. (7) it follows that $B \propto \Delta_E^2$, where in our case by $\Delta_E$ we actually mean the gap at the transition in the average plaquette.

A different, but analogous quantity is the gap of the order parameter, $\Delta$, which can be extracted by looking at the scaling of the maximum of its susceptibility, $\chi$, and using the relation, valid in the large volume limit for a first order transition,

TABLE I. Critical exponents relevant to our analysis.

| | $\nu$ | $\gamma$ | $\alpha$ | $\gamma/\nu$ | $\alpha/\nu$ |
|---|---|---|---|---|---|
| 3D Ising | 0.6301(4) | 1.2372(5) | 0.110(1) | ~1.963 | ~0.175 |
| Tricritical | 1/2 | 1 | 1/2 | 2 | 1 |
| 1st Order | 1/3 | 1 | 1 | 3 | 3 |

$$\chi_{\max} \sim \text{const} + \frac{L_s^3}{4} \Delta^2. \qquad (9)$$

Both $\Delta_E$ and $\Delta$ are expected to vanish as we approach a tricritical mass $m_{\text{tric}}$ from the first order side. In particular, the leading order expected behavior is the following (see [37] or [38] for a brief summary)

$$\Delta_E \propto \sqrt{h - h_{\text{tric}}} \qquad (10)$$

and

$$\Delta \propto \sqrt{|(h - h_{\text{tric}}) \log(h - h_{\text{tric}})|} \qquad (11)$$

where we have indicated generically by $h$ the relevant parameter driving the change from first to second order. It is clear that $h$ is a function of the quark mass and that close enough to the tricritical point one can always set $h - h_{\text{tric}} \sim m - m_{\text{tric}}$; however, appropriate choices of $h$ can improve the region around the tricritical mass where Eqs. (10) and (11) hold. Our choice will be $h \sim m$ in the low mass region and $h \sim 1/m$ in the high mass region. It is interesting to notice that Eq. (11) may seem ambiguous, since a multiplicative redefinition $h \to \text{const} \times h$ changes the functional dependence; however, as long as $(h - h_{\text{tric}}) \ll 1$, the change is subleading and Eq. (11) still gives the dominant contribution.

Close to the tricritical points it can be particularly difficult to discern the correct critical behavior taking place in the thermodynamical limit. Indeed, while first order/3D Ising scaling are expected to take place for a continuous range of values of $m$ and exact tricritical scaling only for specific values $m = m_{\text{tric}}$, what really happens is that tricritical scaling regulates a neighborhood of $m_{\text{tric}}$, whose size goes to zero as $L_s \to \infty$ according to critical indexes known as crossover exponents (see e.g. [34,39,40]). Indeed, the true critical behavior of the system can be seen only for $|t| \lesssim |h - h_{\text{tric}}|^{1/\phi}$, where $t$ is the reduced temperature and $\phi$ is the crossover exponent, which is by definition $\phi = y_h / y_t$ ($y_t$ and $y_h$ are the renormalization group eigenvalues of the relevant variables $t$ and $h - h_{\text{tric}}$), in particular $\phi = 1/2$ in our case [37]. Putting the question the other way around, on a finite lattice of typical size $L_s$, $|t|$ can be traded for $L_s^{-1/\nu}$ and the previous condition becomes $L_s \gtrsim |h - h_{\text{tric}}|^{-\nu/\phi}$; in particular, according to the known tricritical indexes in Table I, one expects tricritical behavior to dominate and mask the correct thermodynamical limit up to a critical size

$$L_c \simeq A|h - h_{\text{tric}}|^{-1}, \qquad (12)$$

where $A$ is some unknown constant. Such a behavior has been studied and verified quantitatively in Ref. [31] in the case of the 3D 3-state Potts model in a negative external field, which shares part of the symmetries studied in the present work.

The difficulties in discerning the correct critical behavior around $m_{tric}$ may result in a difficult determination of the tricritical mass itself. For this reason we have followed the strategy adopted in Ref. [31], i.e. to determine the cumulant of the plaquette $B$ and the gap of the order parameter $\Delta^2$ for values of $m$ where a first order transition is present, and then to determine $m_{tric}$ by fitting data with the expected behaviors reported in Eqs. (10) and (11).

With the aim of determining the tricritical masses $m_{t1}$ and $m_{t2}$ present in the low and high mass regions, respectively, we have studied the critical behavior of the system for various quark masses, $am = 0.005, 0.01, 0.0175, 0.025, 0.03, 0.075, 0.2, 0.5, 1., 1.25, 1.5$ and $2.0$. For each quark mass we have made simulations on lattices with $N_t = 4$ and different spatial sizes $L_s$, reaching up to $L_s = 40$ when necessary to correctly discriminate the critical behavior. Numerical simulations have been performed using the standard Rational Hybrid Monte-Carlo algorithm [41]. Collected statistics have been typically of the order of $10^5$ trajectories around the critical $\beta$ and for each value of $L_s$.

Apart from results obtained for $am = 0.025$ and $am = 0.075$, which were already partially reported in Ref. [16], most numerical simulations have been performed on two GPU farms located in Pisa and Genoa and provided by INFN, consisting of a total of 8 S1070 (32 C1060) NVIDIA GPUs. The numerical code, which runs almost entirely on the GPUs, has been described in detail in Ref. [42].

## III. NUMERICAL RESULTS

The presence of a first order RW endpoint, i.e. of a triple point at the end of the RW lines, has clear signatures in the Monte-Carlo (MC) histories and in the probability distributions of the order parameter and of other quantities. In Fig. 1 we sho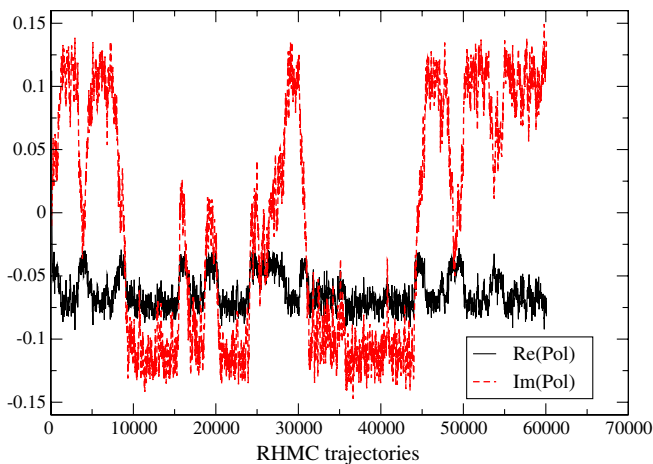w the MC histories of the real and imaginary part of the Polyakov loop for $am = 0.0175$, where the endpoint is first order, and a $\beta$ value around the transition. Metastabilities are clearly detectable, with $Im(L)$, the order parameter, taking three distinct possible values, one in the unbroken and two in the broken $Z_2$ phase. $Re(L)$, which is $Z_2$ even, takes instead only two distinct values corresponding to the broken and unbroken phase.

In Figs. 2–4 we show the reweighted distribution of $Re(L)$, at the pseudocritical values of $\beta$ taking place on the different lattice sizes, for three values of $am$ in the heavy quark region, $am = 1.5, 1.0$ and $0.5$, respectively. For $am = 1.5$ and $am = 1.0$ a double peak distribution clearly develops and deepens as $L_s \to \infty$, indicating a first order transition, even if in the latter case one has to reach $L_s = 40$ to clarify the behavior, indicating that in this case the first order transition is weaker. For $am = 0.5$, instead, the distribution stays single peaked for all explored volumes, suggesting that the endpoint may be second order in this case: this hypothesis is indeed consistent with the determination of $am_{t2}$ presented later.

Similar considerations can be made for the light mass region. In Figs. 5–7 we show the reweighted plaquette distributions at the pseudocritical couplings for $am = 0.005, 0.01$ and $0.075$, respectively. Double peak distributions are present for the two lower masses, with the first order being clearly stronger for $am = 0.005$. For $am = 0.075$ instead, as already shown in Ref. [16], the distribution stays single peaked, suggesting that the endpoint is second order in this case: this is consistent with our determination of $am_{t1}$ (see later).

It is interesting to notice that, when the transition is first order, a gap develops also in other quantities, including the chiral condensate, as visible from Fig. 8, where we show the MC histories of the chiral condensate and of the Polyakov loop around the RW endpoint. That suggests that, as for the usual thermal transition at $\mu = 0$, a strict



FIG. 1 (color online). Monte-Carlo histories of the real and imaginary part of the Polyakov loop for a $\beta$ value (5.328) around the critical point and $am = 0.0175$ on a $16^3 \times 4$ lattice.
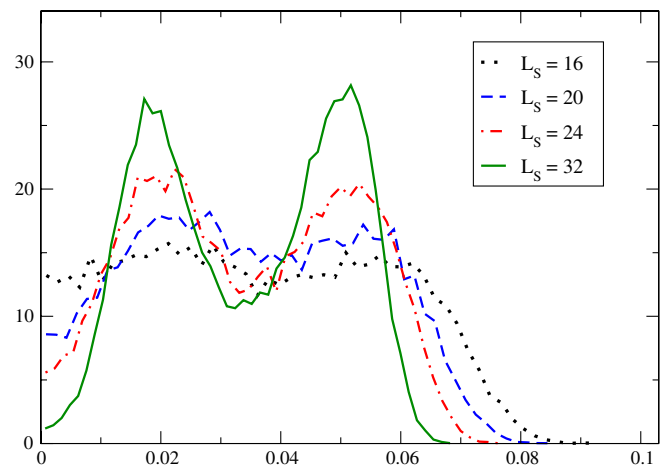


FIG. 2 (color online). Reweighted distribution of the real part of the Polyakov loop at the pseudocritical point for $am = 1.5$ and various lattice sizes.
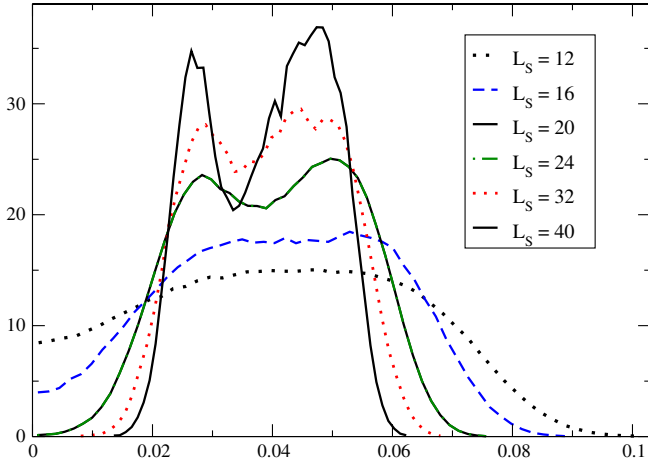
FIG. 3 (color online). Reweighted distribution of the real part of the Polyakov loop at the pseudocritical point for $am = 1.5$ and various lattice sizes.
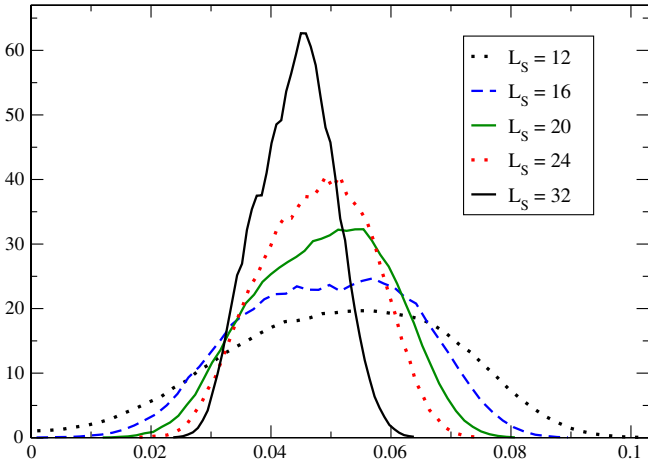


FIG. 4 (color online). Reweighted distribution of the real part of the Polyakov loop at the pseudocritical point for $am = 0.5$ and various lattice sizes.
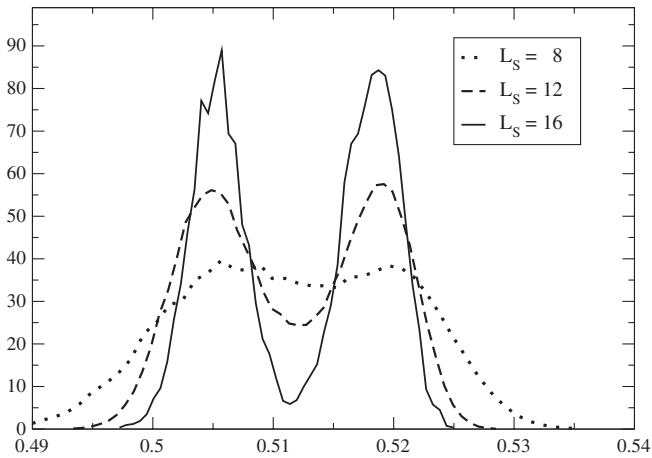


FIG. 5. Reweighted distribution of the plaquette (average of spatial and temporal) at the pseudocritical point for $am = 0.005$ and various lattice sizes.
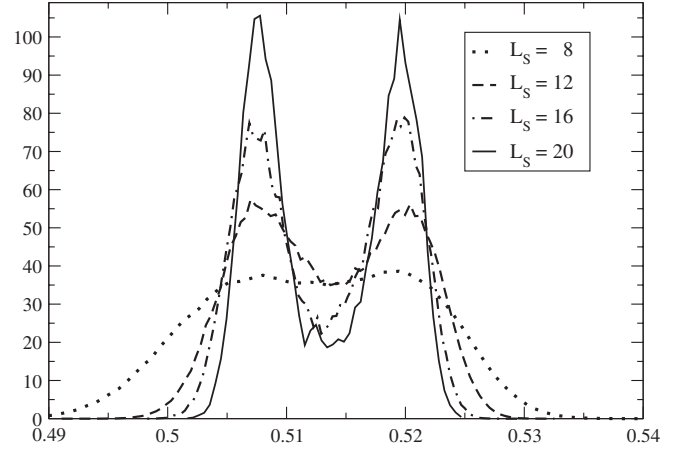


FIG. 6. As in Fig. 5, for $am = 0.01$.
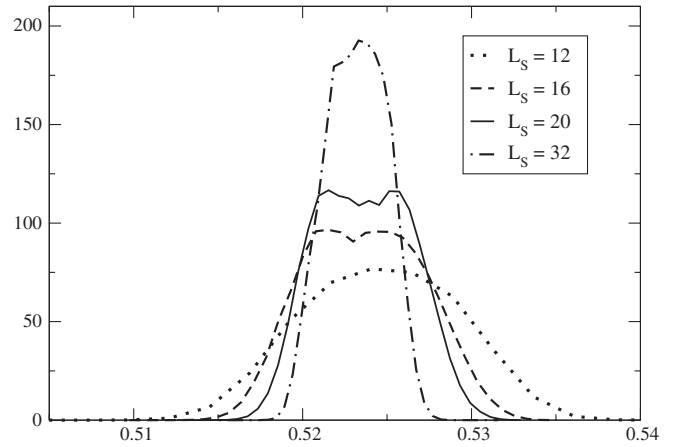


FIG. 7. As in Fig. 5, for $am = 0.075$.

correlation between deconfinement and chiral symmetry restoration may be present also at the RW endpoint.

These results already fully confirm the outcome of Ref. [16]: the RW endpoint is first order in the chiral limit and weakens as the quark mass is increased, until an intermediate mass region is reached where the transition is second order; it is first order again in the high quark mass limit, where it weakens as the quark mass is decreased. The last result is in some sense trivial since, as already discussed in Ref. [16], it is expected from the fact that the $SU(3)$ pure gauge transition is first order.

Further confirmations come from looking at the finite size scaling of the susceptibility of the order parameter, $\chi$, which is shown in Fig. 9 for $am = 0.0175, 0.03, 1.5$ and 1. The first order scaling ansatz, Eq. (5), is always verified for the largest volumes available. However, typically one has to go beyond some critical size before seeing the correct asymptotic critical behavior, and this critical size increases as the transition weakens, i.e. as we approach the tricritical points. For instance, at $am = 1$ first order scaling sets in only for $L_s \geq 32$.
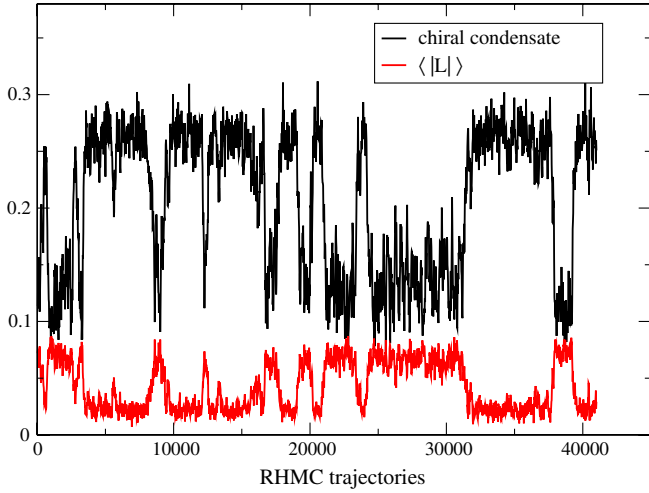
FIG. 8 (color online). Monte-Carlo histories of the Polyakov loop (absolute value) and of the chiral condensate for a $\beta$ value (5.314) around the critical point and $am = 0.01$, on a $16^3 \times 4$ lattice.

Similar considerations apply to the second order region. On the left-hand side of Fig. 10, which is taken from Ref. [16], we show the finite size scaling of $\chi$ for $am = 0.075$ according to 3D Ising critical indexes: scaling is fair for the heights of the peaks and less fair for the widths. On the contrary, we realize that tricritical mean field indexes perform much better, as apparent from the right-hand side of Fig. 10 (notice from Table I that $\gamma/\nu$, regulating the height of the peaks, is practically the same for 3D Ising and tricritical mean field, while $1/\nu$, which regulates the widths of the peaks, is different). That does not mean, of course, that $am = 0.075$ is exactly equal to one of the two tricritical masses, but rather that it is close enough to one of them so that a fake tricritical scaling masks the correct asymptotic scaling at least for sizes up to $L_s = 32$. However, we know neither how close we are to the tricritical mass, nor how large we have to go with $L_s$ to reach the thermodynamical limit, since we have no *a priori* knowledge of the prefactor appearing in Eq. (12).

A quantity which is well suited for discerning 3D Ising from tricritical behavior is the specific heat $C$. Indeed the
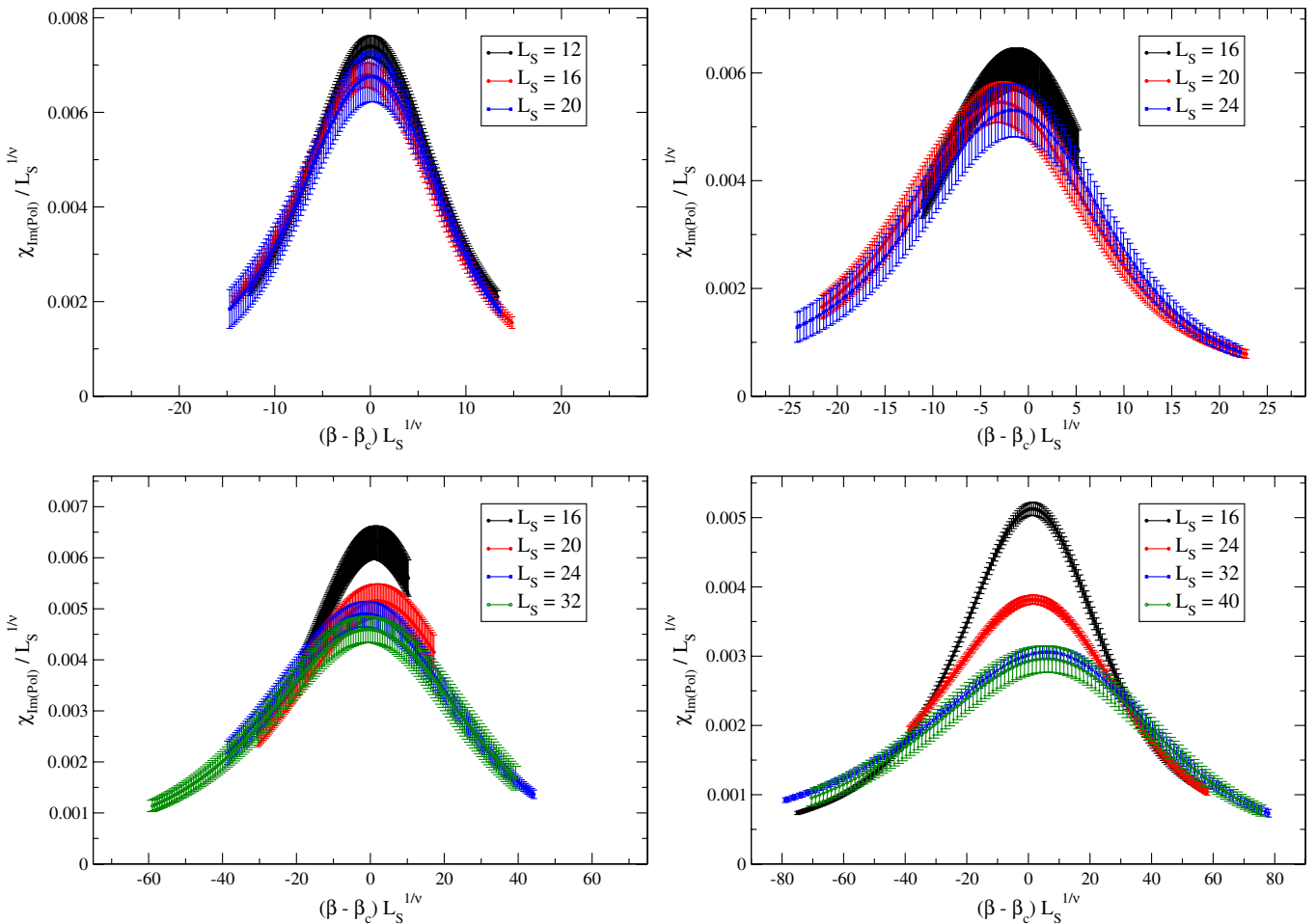


FIG. 9 (color online). Scaling of the reweighted susceptibility of the imaginary part of the Polyakov loop according to first order critical indexes for $am = 0.0175$ (up-left), $am = 0.03$ (up-right), $am = 1.5$ (down-left) and $am = 1.0$ (down-right).
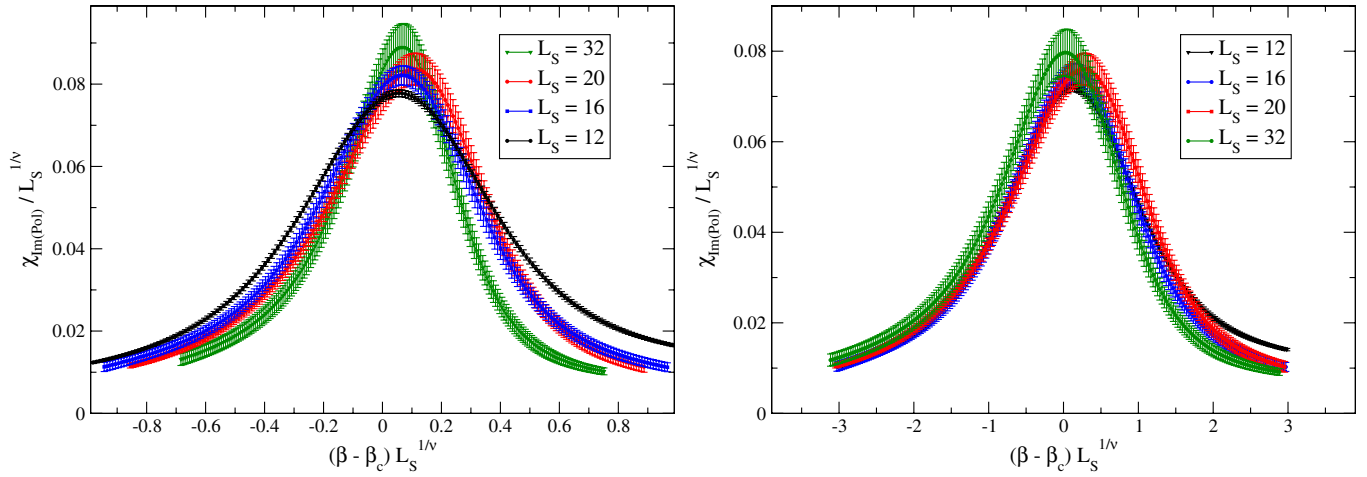
FIG. 10 (color online). Scaling of $\chi$ for $am = 0.075$ according to 3D Ising critical indexes (left) and to tricritical mean field indexes (right).

coefficient $\alpha/\nu$, which regulates the scaling of the height of the singular part of $C$ (see Eq. (6)), changes appreciably when going from tricritical to 3D Ising critical behavior (see Table I), hence deviations from tricritical scaling are expected to appear first in such quantity. A direct measure of the specific heat of the system is not an easy task, however the susceptibility of any quantity, sharing the same transformation properties of the energy under the relevant $Z_2$ symmetry, is expected to scale in the same way: examples are given by the plaquette or by the real part of the Polyakov loop, which are both $Z_2$ even. In Fig. 11 we show the susceptibility of the real part of the Polyakov loop as a function of $L_s$ for $am = 0.2$, which we expect to be in the 3D Ising region. It is apparent that data follow a linear behavior (i.e. $\alpha/\nu = 1$), with deviations visible only for

$L_s \geq 32$ and going in the direction of a smaller value of $\alpha/\nu$ (as expected for 3D Ising); in particular, in the figure we have plotted the result from a linear fit to data up to $L_s = 28$.

Therefore, in order to get a more reliable determination of the tricritical masses, we follow the strategy described in Sec. II and proceed to a determination of the gap of the order parameter and of the plaquette as a function of the quark mass in the first order regions. In Fig. 12 we plot the maxima of the order parameter susceptibility, $\chi$, as a function of $L_s$, for $am = 0.025$, together with a fit to the asymptotic expected behavior, Eq. (9), from which we extract $\Delta^2/4$, The same procedure has been repeated for all quark masses where a first order transition is present. In Fig. 13, instead, we plot the Binder-Challa-Landau
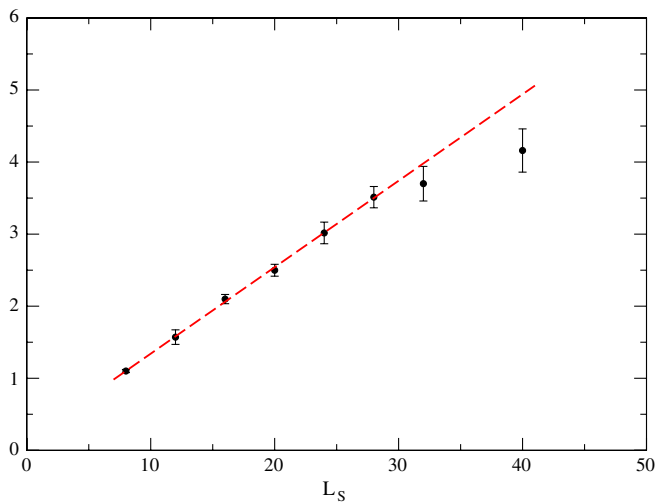


FIG. 11 (color online). Maximum of the susceptibility of the real part of the Polyakov loop as a function of the lattice size $L_s$ and for $am = 0.2$, together with a linear fit including sizes $L_s < 32$.
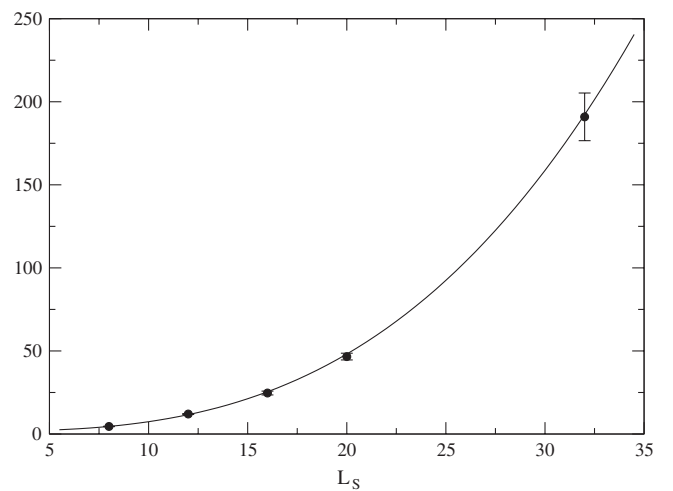


FIG. 12. Maximum of the susceptibility of the order parameter, $\chi$, as a function of the lattice size $L_s$ for $am = 0.025$, together with a cubic fit $\chi = \text{const} + \Delta^2 L_s^3/4$ including all sizes ($\chi^2/\text{d.o.f.} = 0.89$).
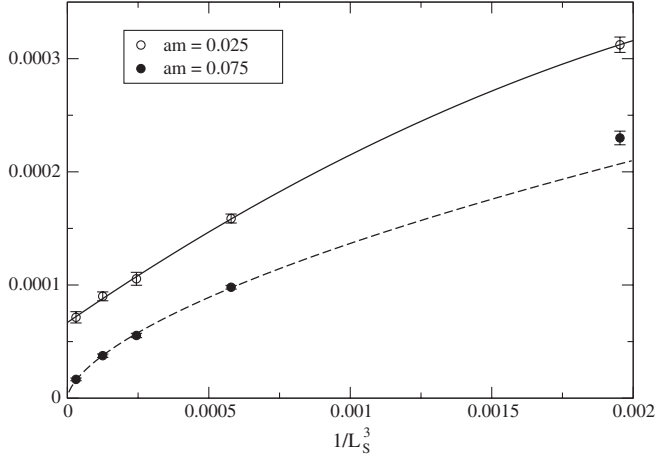
FIG. 13. Binder-Challa-Landau cumulant of the plaquette (see definition in Eq. (8)) as a function of the lattice size for $am = 0.025$ and $am = 0.075$. In the first case a function $B = a + b/L_s^3 + c/L_s^6$ describes well all data with $a = 0.69(4) \times 10^{-4}$ and $\chi^2/\text{d.o.f.} = 0.13$. For $am = 0.075$, instead, data with $L_s > 8$ are well described ($\chi^2/\text{d.o.f.} = 0.69$) by a dependence $B = aL_s^b$ ($b = 0.62(2)$) which gives $B = 0$ in the thermodynamical limit.
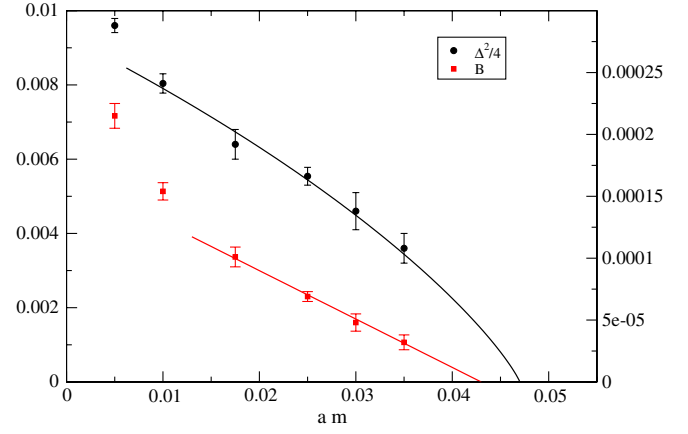


FIG. 14 (color online). Binder-Challa-Landau cumulant of the plaquette, extrapolated to the thermodynamical limit, and $\Delta^2/4$ for small quark masses where a first order transition is present. We include the result from a linear fit $B_\infty = b(am_{t1} - am)$, giving the value of the tricritical mass $am_{t1} = 0.0428(24)$ and $\chi^2/\text{d.o.f.} = 0.13$ (we have included quark masses $am \gtrsim 0.0175$), and from a fit to Eq. (11), $\Delta^2/4 = c(am_{t1} - am)\log(am_{t1} - am)$, giving $am_{t1} = 0.0477(23)$ and $\chi^2/\text{d.o.f.} = 0.37$ (we have included quark masses $am \gtrsim 0.01$).

cumulant of the plaquette, $B$ (see Eq. (8)), as a function of $1/V$ for $am = 0.025$ and $am = 0.075$: in the first case the cumulant extrapolates to a nonzero value as $V \to \infty$, with both linear and quadratic corrections in $1/V$ clearly visible, while in the second case data are well described by a power law and $B = 0$ as $V \to \infty$, indicating the absence of a gap in the plaquette.

In Table II we summarize all determinations obtained for $B$ and $\Delta^2/4$. From such values we can try to determine the tricritical masses as the points where $B$ and $\Delta$ vanish, fitting data to the expected behaviors shown in Eqs. (10) and (11). In Fig. 14 we show the results of such fits in the low mass region for $B$ and $\Delta^2/4$, respectively. We obtain $am_{t1} = 0.0428(24)$ from $B$. Instead, from $\Delta^2/4$, we get

TABLE II. Estimated values for the thermodynamical limit of $B$ and $\Delta^2/4$ for values of the quark mass where a first transition takes place.

| $am$ | $B$ | $\Delta^2/4$ |
|---|---|---|
| 0.005 | $2.15(10) \times 10^{-4}$ | $9.60(20) \times 10^{-3}$ |
| 0.010 | $1.54(7) \times 10^{-4}$ | $8.04(26) \times 10^{-3}$ |
| 0.0175 | $1.01(8) \times 10^{-4}$ | $6.40(40) \times 10^{-3}$ |
| 0.025 | $0.69(4) \times 10^{-4}$ | $5.54(24) \times 10^{-3}$ |
| 0.030 | $0.48(7) \times 10^{-4}$ | $4.60(50) \times 10^{-3}$ |
| 0.035 | $0.32(6) \times 10^{-4}$ | $3.60(40) \times 10^{-3}$ |
| 1.00 | $0.38(4) \times 10^{-5}$ | $2.59(13) \times 10^{-3}$ |
| 1.25 | $0.58(7) \times 10^{-5}$ | $4.16(36) \times 10^{-3}$ |
| 1.50 | $0.66(7) \times 10^{-5}$ | $4.32(24) \times 10^{-3}$ |
| 2.00 | $0.89(7) \times 10^{-5}$ | $5.20(20) \times 10^{-3}$ |

$am_{t1} = 0.0477(23)$ if we fix $h = m$ in Eq. (11), however in this case one should take into account also the systematic uncertainty related to a possible multiplicative redefinition, $h = A_h m$. In order to further check that our results for $B$ and $\Delta^2/4$ can indeed be described in terms of a common tricritical mass, we have also performed a combined fit to all data obtained in the low mass region according to

$$B = b(am - am_{t1})$$
$$\Delta^2/4 = c(am - am_{t1})\log(A_h(am - am_{t1})); \tag{13}$$

including directly, in this case, the possible multiplicative redefinition $h = A_h m$ among the fit parameters. The best fit gives $b = -387(46)$, $c = 0.17(6)$, $A_h = -9(5)$ and $m_{t1} = 0.043(2)$, with a $\chi^2/\text{d.o.f.} = 0.3/4$: the hypothesis is therefore well verified, but we cannot trust the uncertainties on the parameters deriving by this best fit, since data for $B$ and $\Delta^2/4$ are correlated; notice also that the multiplicative constant $A_h$ is poorly determined. Staying conservative with the error estimate, we take as our final determination $m_{t1} = 0.043(5)$.

In Fig. 15 we show instead the same kind of fits for the high mass region: in this case we have used $1/(am)$ as the relevant variable $h$, as explained in Sec. II. We obtain $am_{t2} = 0.71(4)$ from $B$. Instead, regarding $\Delta^2$, we notice that $(h - h_{\text{tric}})$ is $O(1)$ and it makes no sense to look for logarithmic corrections (see Eq. (11)): a simple linear fit for $\Delta^2$ (see Fig. 15) gives $am_{t2} = 0.67(3)$. However, also in this case we can redefine $h = A_h/m$ and try again a combined fit according to
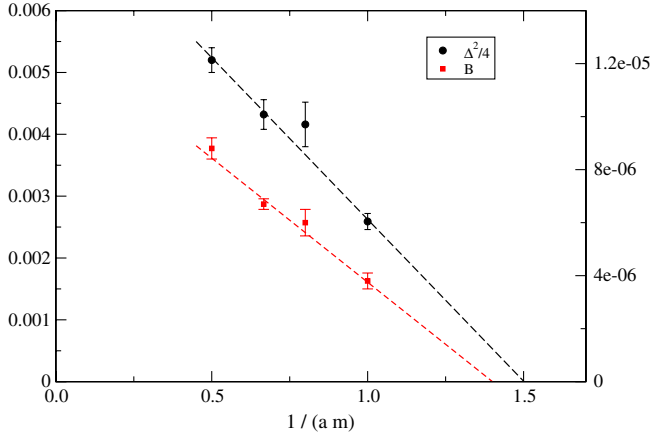
FIG. 15 (color online). Binder-Challa-Landau cumulant of the plaquette, extrapolated to the thermodynamical limit, and $\Delta^2/4$ for high quark masses where a first order transition is present. We include the result from linear fits $B_\infty = b(1/(am_{t2}) - 1/(am))$, giving $am_{t2} = 0.71(4)$ $\chi^2/$d.o.f. $= 1.09$ and $\Delta^2/4 = c(1/(am_{t2}) - 1/(am))$, giving $am_{t2} = 0.67(3)$ ($\chi^2/$d.o.f. $= 1.0$). All masses have been included in the fit in both cases.

$$B = b\left(\frac{1}{am} - \frac{1}{am_{t2}}\right)$$
$$\Delta^2/4 = c\left(\frac{1}{am} - \frac{1}{am_{t2}}\right)\log\left(A_h\left(\frac{1}{am} - \frac{1}{am_{t2}}\right)\right); \tag{14}$$

leading to $am_{t2} = 0.72(5)$ and $A_h \sim 10^{-2}$, with $\chi^2/$d.o.f. $= 2.2/4$. Also in this case one should take into account correlations among data for $B$ and $\Delta^2/4$, hence we prefer to stay conservative in our error estimate and state $am_{t2} = 0.72(8)$.

We notice that both determinations, $am_{t1} = 0.043(5)$ and $am_{t2} = 0.72(8)$, are consistent with the fact that the quark masses for which no metastabilities and double peak distributions are observed ($am = 0.075, 0.2, 0.5$) are within the second order region.

## IV. CONCLUSIONS AND PERSPECTIVES

We have confirmed the outcome of Ref. [16] regarding the order of the endpoint of the RW transition for $N_f = 2$ QCD: a first order endpoint (triple point) is present both in the low mass and in the high mass limit; the endpoint is second order for intermediate quark masses, which are separated from the first order regions by two distinct tricritical masses. Following an investigation performed in Ref. [31] for the 3D 3-state Potts model in a negative external field, which shares part of the same symmetries studied in the present work, we have performed a careful study of some parameters directly linked to the strength of the first order transition, in particular, the Binder-Challa-Landau cumulant of the plaquette and the gap of the order parameter; that has permitted to obtain independent and

consistent determinations of the two tricritical masses. Staying conservative with error estimates, we state as our final result $am_{t1} = 0.043(5)$ and $am_{t2} = 0.72(8)$. Such results are summarized in Fig. 16, where we sketch a phase diagram in the $T$-$m_q$ plane.

The value of $am_{t1}$ corresponds to a pion mass of the order of 400 MeV, hence we conclude that for physical quark masses the RW endpoint should be well inside the first order region. It is therefore of primary importance to explore what is the fate of the further first order lines departing from the triple point. One of them, in particular, may reach the zero density axis or have a critical endpoint arbitrarily close to it, which could have great influence on the physics of strongly interacting matter right above the deconfinement transition. The question is also strictly connected to the problem of the order of the chiral transition for $N_f = 2$ [43,44].

Another important issue is of course to extend our investigation to $N_f \neq 2$ and confirm the conjecture that the nature of the transition at $\mu = 0$ may be regulated by the physics of the RW endpoint [16], i.e. that the $\mu = 0$ transition is first order only when the first order line departing from the RW triple point reaches the $\mu = 0$ axis, and that tricritical scaling indeed shapes the chiral critical surface [19].

All these investigations will require extensive numerical simulations, which are however perfectly feasible since they involve an imaginary chemical potential. Part of this program is progress.

We stress that our present results are valid for the standard rooted staggered discretization of the theory and for lattices with $N_t = 4$, corresponding to a lattice spacing of about 0.3 fm. A key issue is then also to verify that the main features of the phase diagram remain unchanged
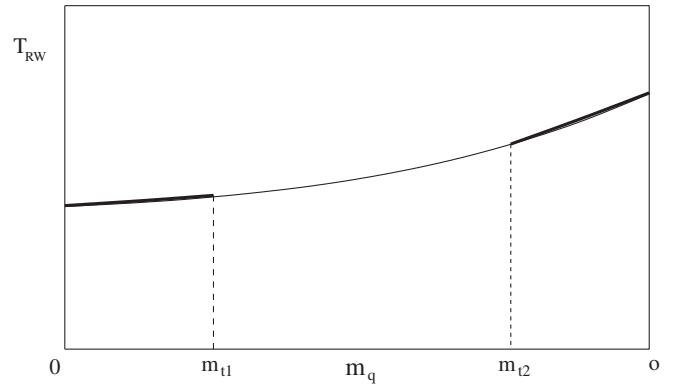


FIG. 16. Sketch of the phase diagram in the $T$-$m_q$ plane which summarizes our results: in $N_f = 2$ QCD the endpoint of the Roberge-Weiss transition is first order close to the chiral and to the quenched limit and second order for intermediate masses. A conservative estimate for the two tricritical masses separating the second order region from the first order ones, for the lattice discretization adopted in the present work, is $am_{t1} = 0.043(5)$ and $am_{t2} = 0.72(8)$.

when changing discretization and/or approaching the continuum limit. The two tricritical masses could still be present, but the first order regions could in principle extend or shrink in a significant way.

[1] M. G. Alford, A. Kapustin, and F. Wilczek, Phys. Rev. D **59**, 054502 (1999).

[2] M. P. Lombardo, Nucl. Phys. B, Proc. Suppl. **83**, 375 (2000).

[3] P. de Forcrand and O. Philipsen, Nucl. Phys. **B642**, 290 (2002).

[4] P. de Forcrand and O. Philipsen, Nucl. Phys. **B673**, 170 (2003).

[5] M. D'Elia and M. P. Lombardo, Phys. Rev. D **67**, 014505 (2003); **70**, 074509 (2004).

[6] V. Azcoiti, G. Di Carlo, A. Galante, and V. Laliena, Nucl. Phys. **B723**, 77 (2005).

[7] H. S. Chen and X. Q. Luo, Phys. Rev. D **72**, 034504 (2005).

[8] P. Giudice and A. Papa, Phys. Rev. D **69**, 094509 (2004).

[9] P. Cea, L. Cosmai, M. D'Elia, and A. Papa, J. High Energy Phys. 02 (2007) 066.

[10] M. D'Elia, F. Di Renzo, and M. P. Lombardo, Phys. Rev. D **76**, 114509 (2007).

[11] S. Conradi and M. D'Elia, Phys. Rev. D **76**, 074501 (2007).

[12] P. Cea, L. Cosmai, M. D'Elia, and A. Papa, Phys. Rev. D **77**, 051501(R) (2008).

[13] M. D'Elia and F. Sanfilippo, Phys. Rev. D **80**, 014502 (2009).

[14] P. Cea, L. Cosmai, M. D'Elia, C. Manneschi, and A. Papa, Phys. Rev. D **80**, 034501 (2009).

[15] P. Cea, L. Cosmai, M. D'Elia, and A. Papa, Phys. Rev. D **81**, 094502 (2010).

[16] M. D'Elia and F. Sanfilippo, Phys. Rev. D **80**, 111501(R) (2009).

[17] H. Kouno, Y. Sakai, K. Kashiwa, and M. Yahiro, J. Phys. G **36**, 115010 (2009).

[18] Y. Sakai, H. Kouno, and M. Yahiro, J. Phys. G **37**, 105007 (2010).

[19] P. de Forcrand and O. Philipsen, Phys. Rev. Lett. **105**, 152001 (2010).

[20] G. Aarts, S. P. Kumar, and J. Rafferty, J. High Energy Phys. 07 (2010) 056.

[21] A. Roberge and N. Weiss, Nucl. Phys. **B275**, 734 (1986).

[22] T. DeGrand and R. Hoffmann, J. High Energy Phys. 02 (2007) 022.

[23] T. DeGrand, R. Hoffmann, and J. Najjar, J. High Energy Phys. 01 (2008) 032.

[24] B. Lucini, A. Patella, and C. Pica, Phys. Rev. D **75**, 121701 (2007).

[25] B. Lucini and A. Patella, Phys. Rev. D **79**, 125030 (2009).

[26] J. C. Myers and M. C. Ogilvie, J. High Energy Phys. 07 (2009) 095.

[27] A. Armoni, M. Shifman, and G. Veneziano, Phys. Rev. Lett. **91**, 191601 (2003).

[28] M. Unsal and L. G. Yaffe, Phys. Rev. D **74**, 105019 (2006).

[29] Y. Sakai, T. Sasaki, H. Kouno, and M. Yahiro, Phys. Rev. D **82**, 076003 (2010).

[30] P. de Forcrand and O. Philipsen, J. High Energy Phys. 01 (2007) 077; 11 (2008) 012.

[31] C. Bonati and M. D'Elia, Phys. Rev. D **82**, 114515 (2010).

[32] S. Kim, Ph. de Forcrand, S. Kratochvila, and T. Takaishi, Proc. Sci., LAT2005 (2006) 166 [arXiv:1010.3639].

[33] L. D. Landau and E. M. Lifshitz, *Statistical Physics, Part 1* (Butterworth Heinemann, London, 1980).

[34] A. Pelissetto and E. Vicari, Phys. Rep. **368**, 549 (2002).

[35] M. S. S. Challa, D. P. Landau, and K. Binder, Phys. Rev. B **34**, 1841 (1986).

[36] J. Lee and J. M. Kosterlitz, Phys. Rev. B **43**, 3265 (1991).

[37] I. D. Lawrie and S. Sarbach, in *Theory of Tricritical Points*, edited by C. Domb and J. L. Lebowitz (Academic Press, New York, 1987), Vol. 11.

[38] D. E. Sheehy, Phys. Rev. A **79**, 033606 (2009).

[39] K. Binder and H. P. Deutsch, Europhys. Lett. **18**, 667 (1992).

[40] J. Cardy, *Scaling and Renormalization in Statistical Physics* (Cambridge University Press, Cambridge, England, 2003).

[41] A. D. Kennedy, I. Horvath, and S. Sint, Nucl. Phys. B, Proc. Suppl. **73**, 834 (1999).

[42] C. Bonati, G. Cossu, M. D'Elia, and A. Di Giacomo, Proc. Sci. LAT2010 (2010) 324 [arXiv:1010.5433].

[43] M. D'Elia, A. Di Giacomo, and C. Pica, Phys. Rev. D **72**, 114510 (2005).

[44] G. Cossu, M. D'Elia, A. Di Giacomo, and C. Pica, arXiv:0706.4470.